

AD-765 478

COMBINED STRESS STRENGTH RESULTS FOR A  
HIGH-PURITY, SLIP-CAST FUSED SILICA

Richard E. Ely

Army Missile Command  
Redstone Arsenal, Alabama

16 July 1973

DISTRIBUTED BY:

**NTIS**

National Technical Information Service  
U. S. DEPARTMENT OF COMMERCE  
5285 Port Royal Road, Springfield Va. 22151

AD 765478

AD

TECHNICAL REPORT

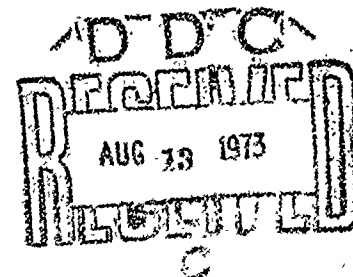
RR-73-7

COMBINED STRESS STRENGTH RESULTS FOR  
A HIGH-PURITY, SLIP-CRYSTAL  
FUSED SILICA

by

Richard E. Ely

July 1973



Approved for public release; distribution unlimited.



**U.S. ARMY MISSILE COMMAND**

*Redstone Arsenal, Alabama*



UNCLASSIFIED  
Security Classification

DOCUMENT CONTROL DATA - R & D		
(Security classification of title, body of abstract and indexing annotation must be entered when the overall report is classified)		
1. ORIGINATING ACTIVITY (Corporate author) US Army Missile Research, Development and Engineering Laboratory US Army Missile Command Redstone Arsenal, Alabama 35809		2a. REPORT SECURITY CLASSIFICATION UNCLASSIFIED
		2b. GROUP NA
3. REPORT TITLE  COMBINED STRESS STRENGTH RESULTS FOR A HIGH-PURITY, SLIP-CAST FUSED SILICA		
4. DESCRIPTIVE NOTES (Type of report and inclusive dates) Technical Report		
5. AUTHOR(S) (First name, middle initial, last name)  Richard E. Ely		
6. REPORT DATE 16 July 1973	7a. TOTAL NO. OF PAGES 28-27	7b. NO. OF REFS 8
8a. CONTRACT OR GRANT NO.  a. PROJECT NO. (DA) 1T062106A330  c. AMC Management Structure Code 502E.11.29600  d.		8b. ORIGINATOR'S REPORT NUMBER(S) RR-73-7
		8c. OTHER REPORT NO(S) (Any other numbers that may be assigned this report) AD
10. DISTRIBUTION STATEMENT  Approved for public release; distribution unlimited.		
11. SUPPLEMENTARY NOTES  None		12. SPONSORING MILITARY ACTIVITY  Same as No. 1
13. ABSTRACT  A pressure vessel test method was used to fracture tubular specimens of a high-purity, slip-cast fused silica under ten biaxial stress states. The hoop tensile strengths obtained were from 2990 to 4300 psi. The uniaxial compressive strengths ranged from -25,800 to -48,800 psi. Different material lots were employed and strength variation with lot were observed. The modulus of rupture, 5365 psi, also was determined for 3/4-inch diameter rods.		

DD FORM 1473  
1 NOV 65

REPLACES DD FORM 1473, 1 JAN 64, WHICH IS  
OBSOLETE FOR ARMY USE.

UNCLASSIFIED

Security Classification

UNCLASSIFIED

Security Classification

14. KEY WORDS	LINK A		LINK B		LINK C	
	ROLE	WT	ROLE	WT	ROLE	WT
Slip-cast fused silica Biaxial stress tests Specimen-pistons assembly Cylindrical pressure vessel						

UNCLASSIFIED

Security Classification

///

## CONTENTS

	Page
1. Introduction . . . . .	2
2. Test Procedure . . . . .	2
3. Results . . . . .	5
4. Discussion . . . . .	6
References . . . . .	23

## 1. Introduction

Slip-cast fused silica (SCFS) is one of few materials that is suitable for use in radome and leading-edge missile and rocket applications above Mach 5 [1]. It has been chosen as the best state-of-the-art material for radar experiments where velocities up to Mach 8 could be experienced [2], even though it is recognized that improvements are needed in its ablation and rain erosion resistance.

In order to assist in developing sound structural designs with SCFS, the strength behavior of a high purity material was determined under ten biaxial stress states at room temperature. Modulus of rupture data also were determined.

## 2. Test Procedure

### a. Apparatus

All flexure and biaxial stress tests were conducted at room temperature. Four point loading was employed to conduct the flexure tests. The upper and lower breaking spans were 2 and 4 inches, respectively. The test specimens were precision machined circular rods (Paragraph 2.b.).

The "pressure vessel" test method has been employed previously [3]. The pressure vessel apparatus consists primarily of a specimen-pistons assembly (Figure 1) which is inserted into a cylindrical pressure vessel (Figure 2). During testing, this apparatus is located on the weighing table of a universal tester where the tester is used for measuring loads generated by the apparatus. The specimen had aluminum plug-type, end adapters which were cemented to the specimen ID surface with epoxy resin (Figure 3). The plug insertion length was 1 inch. For all tests, the end adapters also include an aluminum end ring (not shown) which is cemented to the OD surface of the specimen and where the ring length matched the plug length. Each end adapter has a central hole which mates with a piston shaft (Figure 3) in order to insure alignment; alignment also was maintained using these holes and suitable fixtures during assembly of the specimen and end adapters [3]. The piston diameters were 3 inches.

The operating principle of the pressure vessel apparatus is similar to that used in other studies [4, 5]. Specimen loading (Figure 2) was accomplished by various combinations of internal fluid pressure,  $p_i$ , external fluid pressure,  $p_o$ , and pressure,  $p_z$ , which is applied to the lower surface of the bottom piston. For the present study, only one or two of the volumes were pressurized for a test. Discrete pressure ratios were obtained using booster assemblies (not shown) so that the

biaxial loading was applied in a proportional manner during a test for 9 of the 10 loading paths employed. Being able to measure axial loads externally is a unique feature of the apparatus and this capability provided a means for evaluating the frictional forces on the top piston when rubber O-ring seals were used ( $P_o > 0$ ); corrections for the frictional forces were small [3]. The primary pressure source was bottled nitrogen gas; water was used as a secondary pressure source. Pertinent pressures were recorded as a function of time and maximum pressures were measured with bourdon tube type dial gages.

#### b. Test Specimens

All test specimens were procured as finished items\*. The starting material specified was high purity silica slip, WS-8442, Type III or equal in accordance with the Department of Navy, Weapons Specification WS-8429, Grade B. Specimen requirements were:

Composition, percent . . . . .	99.5 + silica
Density, gm/cc . . . . .	2.00 ± 0.10
Porosity, percent maximum . . . . .	14.0
Modulus of Rupture at 75°F, psi, minimum . . . . .	4000

The sixty biaxial stress specimens were supplied in five lots which were designated as 4A, 5A, 6A, 7A, and 8A; the number of specimens for each lot were 15, 26, 8, 9, and 2, respectively. Production dates for these lots extended over a period of 30 days. The twelve flexure specimens were of a single lot.

The flexure specimens were circular rods which had a nominal diameter of 0.730 inch and a length of 5 inches; a maximum surface roughness of 32 microinches was specified. For biaxial stresses, the test specimens were uniform, thin-walled tubes which had a 1.186-inch ID, a 0.075-inch wall, and a length of 3.500 inches. The specimen gage length was 1.500 inches or 2 inches less than the total length because of the end adapters. The maximum surface roughness specified for the internal and external surfaces was 32 microinches.

#### c. Stress Calculations

All stresses were computed using the initial dimensions of the test specimens. Hoop stresses were computed for the ID surface

---

\*The Burnswick Corporation, Marion, Virginia



using the thick-walled formula. For hoop tension stress the expression was

$$\sigma_t = \frac{p_i (D^2 + d^2)}{(D^2 - d^2)} \quad (1)$$

and for hoop compression stress,

$$\sigma_t = \frac{-2p_o D^2}{(D^2 - d^2)} \quad (2)$$

where

$p_i$  = internal pressure

$p_o$  = external pressure

$D$  = specimen OD

$d$  = specimen ID.

The axial stress was calculated by three expressions depending upon the stress state or pressure loading.

When pressures  $p_i$  and  $p_o$  were used (Figure 2), the axial stress was computed using

$$\sigma_z = \frac{p_o (A^2 - D^2) + p_i d^2 - \left(\frac{4}{\pi}\right) f}{D^2 - d^2} \quad (3)$$

For pressures  $p_i$  and  $p_z$ ,

$$\sigma_z = \frac{p_i d^2 - \left(\frac{4}{\pi}\right) (L)}{D^2 - d^2} \quad (4)$$

and for pressures  $p_o$  and  $p_z$

$$\sigma_z = \frac{p_o (A^2 - D^2) - \left(\frac{4}{\pi}\right) (L + f)}{D^2 - d^2} \quad (5)$$

where  $L$  is measured axial load,  $f$  the frictional load (experimental), and  $A$  the ID of pressure vessel. In Equations (3) and (5) the friction load was taken as zero when  $p_o = 0$  since no rubber O-ring seals were used on the top piston (Figure 2).

### 3. Results

A high-purity SCFS was tested in flexure and under biaxial stresses at room temperature. The average modulus of rupture obtained for 12 tests (Table 1) was 5365 psi. Breaking times ranged from approximately 60 to 120 seconds. The density measured for the flexure specimen was 1.88 gm/cc using ASTM Method C373-56.

Combined stress strength results for the SCFS are presented in Table 2 for 57 tests. The data were tabulated in the same order as the stress states or loading paths were numbered (Figure 4). All of the biaxial loading was proportional except for path number 10. Fracture times were longest for uniaxial compression and compression-compression (CC) stresses (Table 2). The estimated density for Lot 5A was 1.92 gm/cc; ASTM Method C373 was used but samples weighed much less than 50 gm.

A strength variation with material lot was obtained (Table 2). Lot 5A, for example, was tested at least twice for each stress state; the strength magnitudes were never the maximum but rather were the minimum for 8 of the 10 stress states. On the other hand, the strength magnitudes for Lot 6A (8 specimens) were maximum values for 6 of 8 stress states and were never a minimum value.

The strength results for all 57 biaxial stress tests are plotted in Figure 5. The envelope shown contains all but two of the data points. For uniaxial tension, the bounds of this envelope were 2370 and 4360 psi giving a median tensile strength of 3365 psi. The average compressive strength for all material lots was -37,000 psi; the greatest compressive strength was -48,800 psi for Lot 6A while the lowest was -25,800 psi for Lot 5A.

The strength data for Lot 6A material were not only the greatest in magnitude, generally, but they also exhibited a definite trend (Figure 6). Results for these eight tests compare quite favorably with the strength predictions of the Leon Theory [6], a generalized shear-stress, internal friction criterion [3]. The theoretical curve was constructed using a tensile strength,  $\sigma_o$ , of 4200 psi and a  $k$  ratio (absolute ratio of compressive-to-tensile strength) of 11.62. The theoretical curve (Figure 6) also would serve as the outer boundary or envelope for all of the data (Figure 5). Another theory which would fit these data reasonably well is the modified maximum strain energy theory [7], using a Poisson's ratio of 0.15 [1].

The SCFS fractured in a brittle manner for all stress states. For loading paths 1 and 2 (Figure 4), the fracture mode was most often a transverse break (Figure 7); these breaks occurred both at and away from the end adapter. Near equal biaxial tension stresses (path number 3), the specimens broke into small and large pieces of irregular shapes (Figure 8a). For loading paths 4 and 5 (Figures 8b and 8c), the specimens broke into powder and small pieces. For path 6 (Figure 8d) the fracture mode changed into many small pieces which had approximate rectangular shapes. For paths 7, 8, 9, and 10, the specimen remains again consisted of small pieces and powder.

#### 4. Discussion

The strength magnitudes obtained for the high-purity SCFS compare reasonably well with results reported for other studies; however, a word of caution is offered before presenting these data comparisons. Strength data obtained for SCFS can be influenced both by material and test method differences [1]. Two important material differences include the density and microstructure where both can be significantly altered by the degree of sintering. Included under test method differences are size effects and specimen surface finish.

Southern Research Institute (SRI) has reported tensile strengths for high-purity SCFS of 2200 to 4300 psi [1]; "dog bone" type specimens were axially loaded. The Georgia Institute of Technology reported average values of 2568, 3135, and 3863 psi using hydrostatic tensile rings of three sizes and where the strength increased with decreasing ring volume [1]. In the current biaxial stress study, the axial tensile strength (path 2) varied from 2450 to 4120 psi and the hoop tensile strength (path 5) varied from 2990 to 4300 psi; in both cases the higher value was for Lot 6A material and the lower value for Lot 5A. The average of all axial and hoop tensile data was 3439 psi.

SRI also reported compressive strength values for high purity SCFS which ranged from about -30,000 to -54,000 psi. Values in the current study ranged from -25,800 psi for Lot 5A material to -48,800 psi for one test with Lot 6A material. Material differences existed for the two studies.

Modulus of rupture data are compared in Table 3. These data demonstrate that strength variations do result from differences in surface finish as well as density. The current value, 5365 psi, appears reasonable for a ground surface and the relatively low, 1.92 gm/cc, density.

The Leon Theory also has been used to correlate data for a high density graphite [3] and aluminum silicate [8].

TABLE 1. MODULUS OF RUPTURE OF HIGH-PURITY,  
SLIP-CAST FUS<sup>2</sup>O SILICA

Test No.	Modulus of Rupture (psi)
1	5910
2	5950
3	5850
4	5520
5	2570
6	3460
7	5810
8	6330
9	5530
10	6550
11	4680
12	6220
	5365 ± 1213*

\*Estimated standard deviation

TABLE 2. COMBINED STRESS STRENGTH RESULTS FOR A  
HIGH-PURITY, SLIP-CAST FUSED SILICA

Test No.	Lot No.	Hoop Stress (psi)	Axial Stress (psi)	Fracture Time (sec)
T1833	5A	-1810	3460	48
T1835	5A	-1740	3310	29
T1857	4A	-1490	2810	17
T1853	8A	-1960	3770	21
T1880	7A	-1040	1900	24
T1881	8A	-2040	3920	17
T1873	4A	-115	2520	12
T1874	5A	-160	3550	43
T1875	5A	-112	2450	25
T1876	6A	-185	4120	42
T1877	7A	-144	3180	23
T1843	5A	2180	2370	65
T1844	5A	2610	2920	38
T1857	6A	2240	2450	30
T1858	7A	2870	3280	42
T1859	4A	2100	2260	38
T1836	5A	2770	1220	38
T1837	5A	4190	1850	75
T1854	4A	4280	1890	58
T1855	6A	4050	1790	60
T1856	7A	2900	1280	47
T1845	5A	3140	-384	--
T1846	5A	2990	-390	--
T1860	4A	4010	-506	44
T1861	6A	4300	-638	48
T1862	7A	4130	-480	58

TABLE 2. CONTINUED.

Test No.	Lot No.	Hoop Stress (psi)	Axial Stress (psi)	Fracture Time (sec)
T1839	5A	3560	-8060	82
T1840	5A	2760	-6230	61
T1841	5A	2120	-7900	72
T1842	5A		-8600	72
T1843	5A		-10200	87
			-12900	42
		1110	-13200	45
T1870	5A	2860	-12000	36
T1871	6A	3620	-15300	44
T1872	7A	3510	-15200	56
T1863	4A	2830	-33000	63
T1864	5A	2450	-28800	47
T1865	5A	2020	-24100	45
T1866	6A	3080	-36400	121
T1867	7A	2590	-31100	
T1841	5A	--	-33200	253
T1842	5A	--	-25800	102
T1849	6A	--	-48800	156
T1850	4A	--	-37800	29
T1851	7A	--	-39400	51
T1887	5A	--	-32100	102
T1888	5A	--	-32300	66
T1889	5A	--	-44900	96
T1890	4A	--	-33000	97
T1891	4A	--	-41900	71
T1892	4A	--	-38000	115

TABLE 2. CONCLUDED

Test No.	Lot No.	Hoop Stress (psi)	Axial Stress (psi)	Fracture Time (sec)
T1882	5A	-5190	-41800	285*
T1883	5A	-5280	-40900	187*
T1884	4A	-5280	-44200	140*
T1885	4A	-5380	-38600	112*
T1886	5A	-5380	-34000	147*

\*Nonproportional loading.

TABLE 3. MODULUS OF RUPTURE FOR SCFS, ROUND SPECIMENS,  
2/4, UPPER/LOWER BREAKING SPANS

Density (gm/cc)	Surface Finish	Specimen Diameter (in.)	Modulus of Rupture (psi)
2.06	As cast	0.75	4597*
1.96	As cast	0.75	4860*
1.92***	Ground	0.73	5365**
2.06	Ground and Polished	0.6	5920*

\*Reference [1]

\*\*Current Study

\*\*\*Estimated, see text



Figure 1. Specimen-pistons assembly.



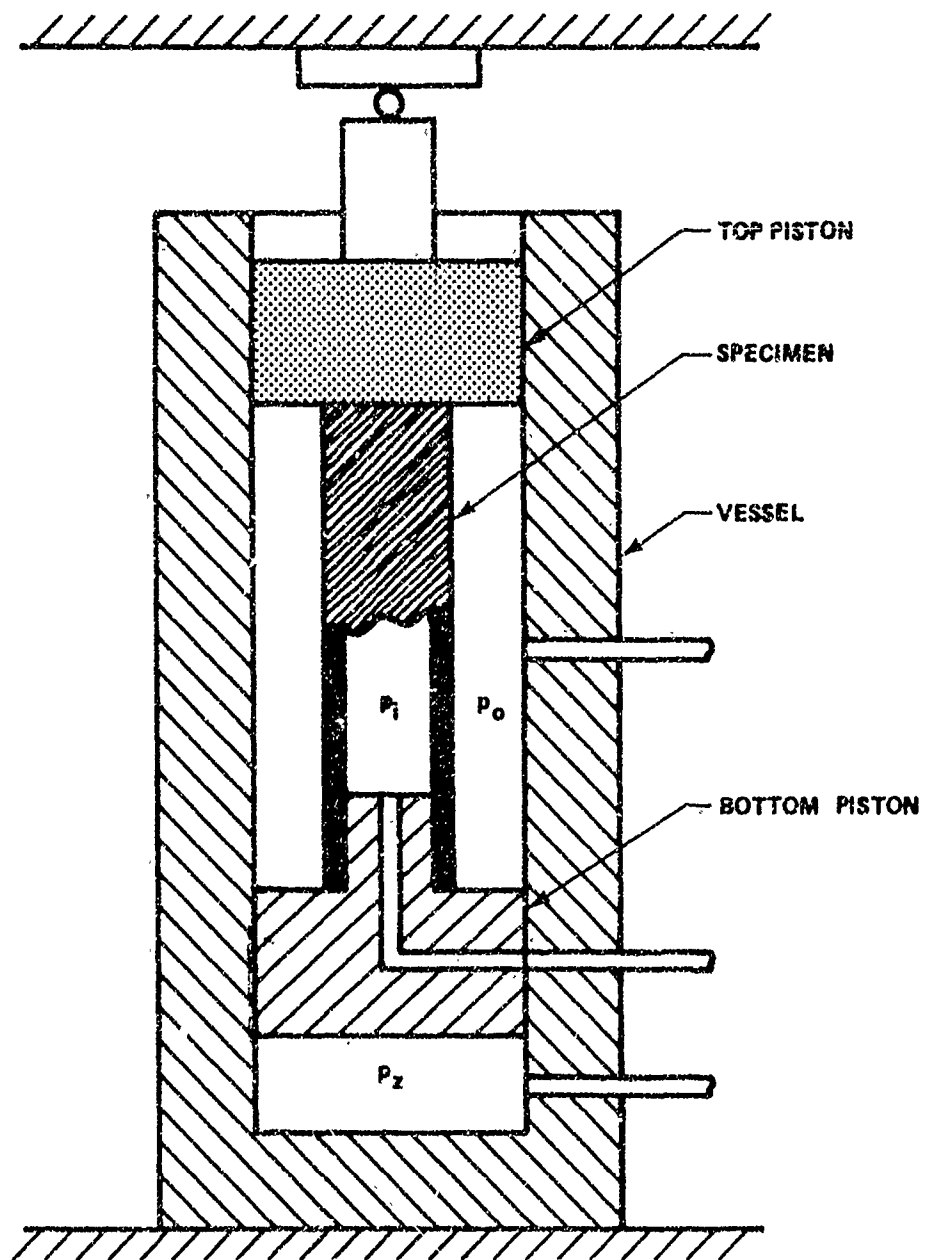


Figure 2. Schematic of apparatus.

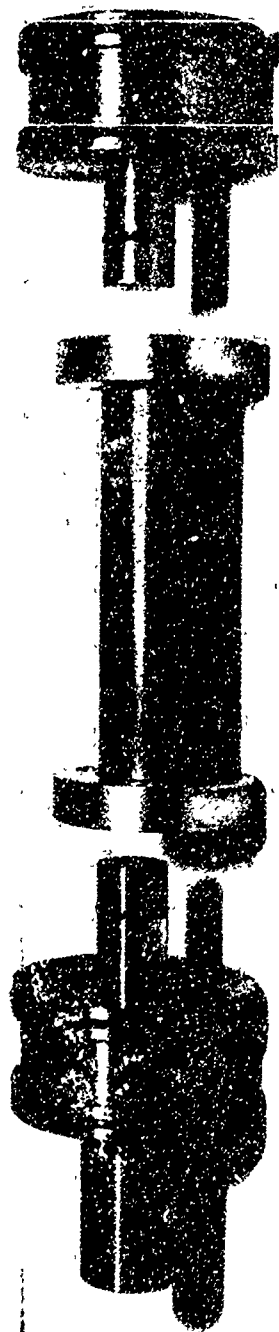


Figure 3. Pistons and specimen-adapters assemblies.

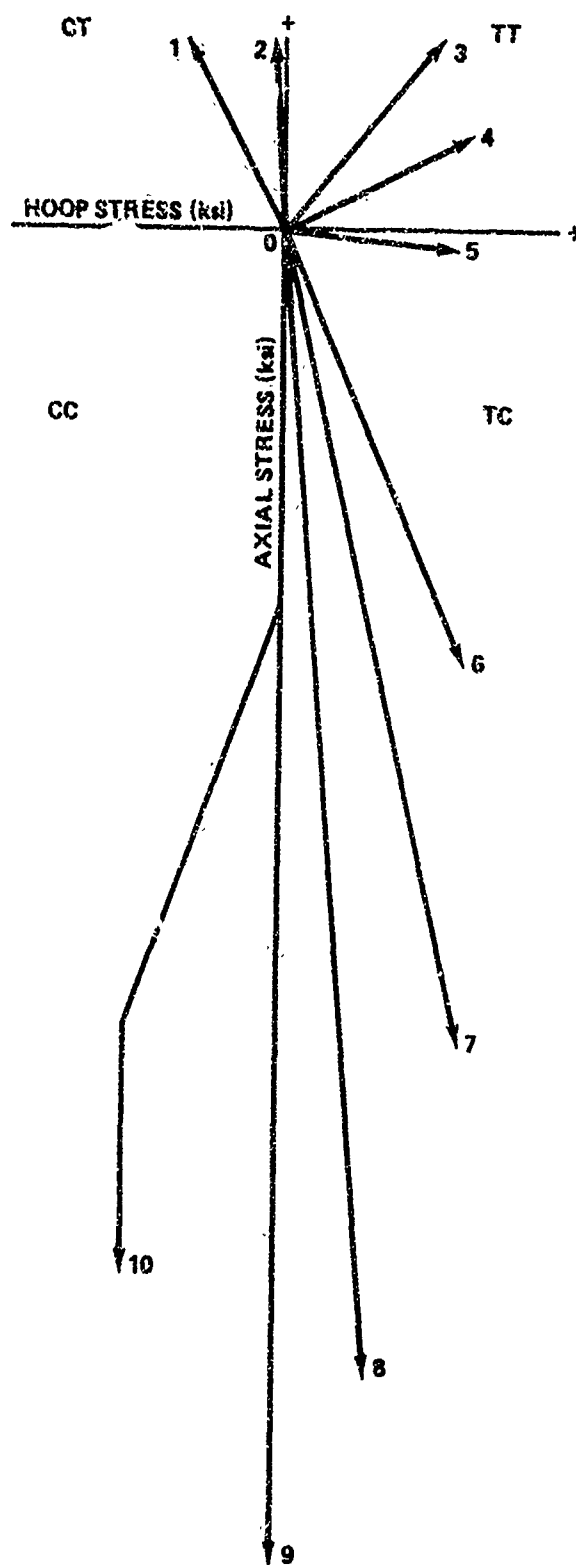


Figure 4. Loading paths employed.

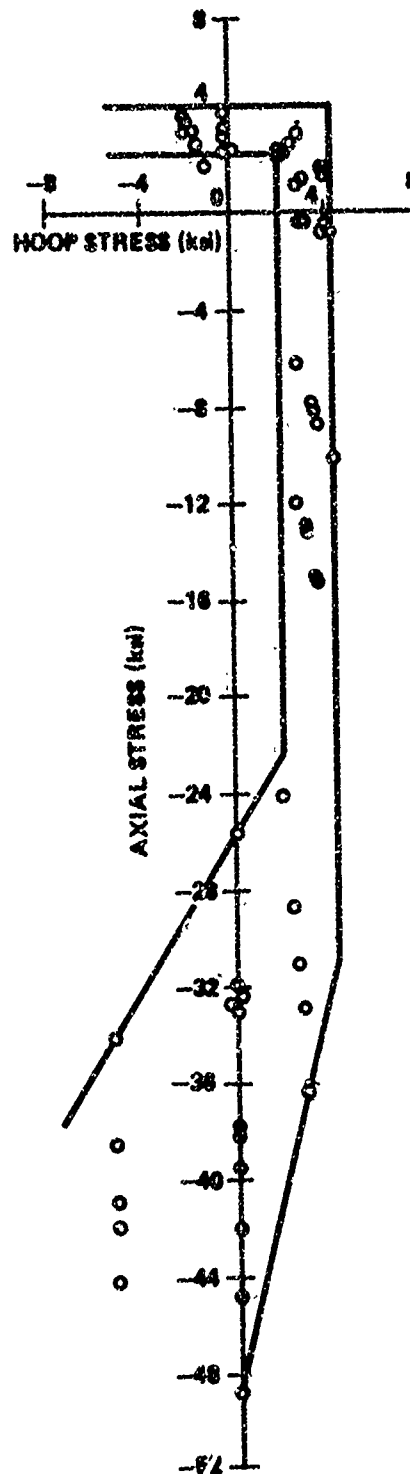


Figure 5. SCFS strength results for all tests.

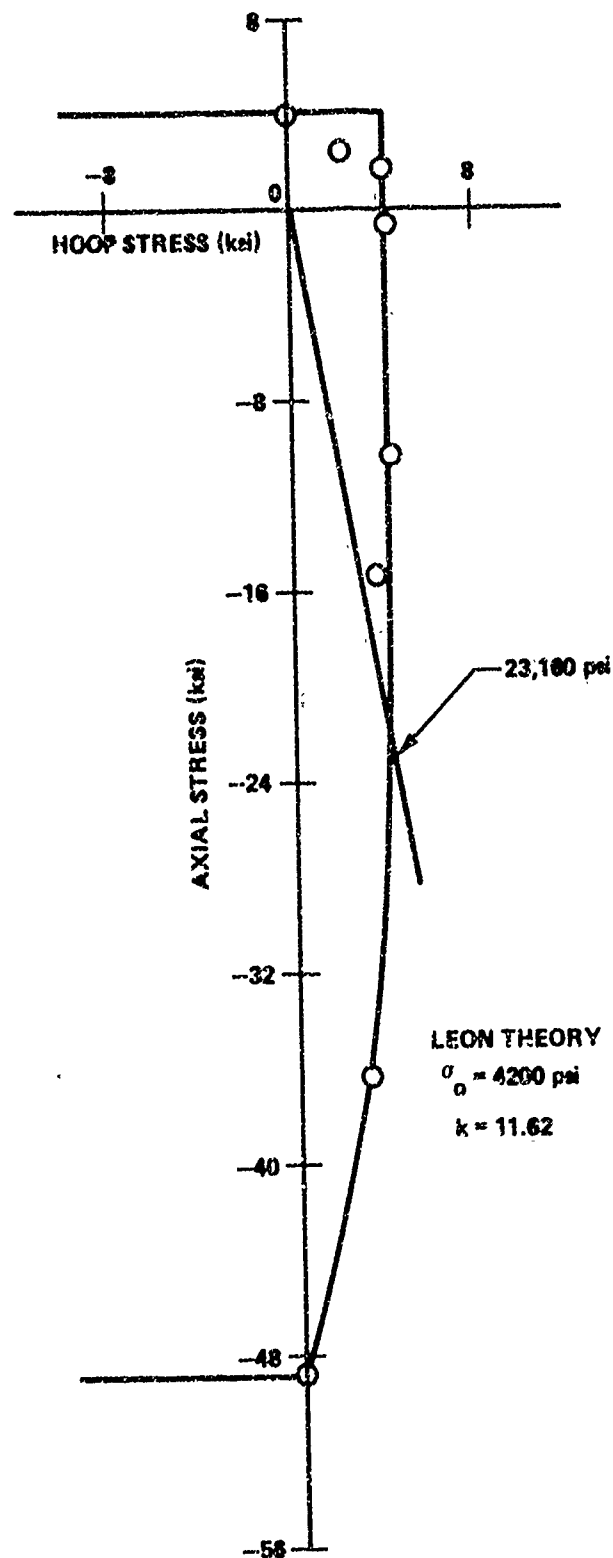


Figure 6. SCFS strength results for Lot 6A material.

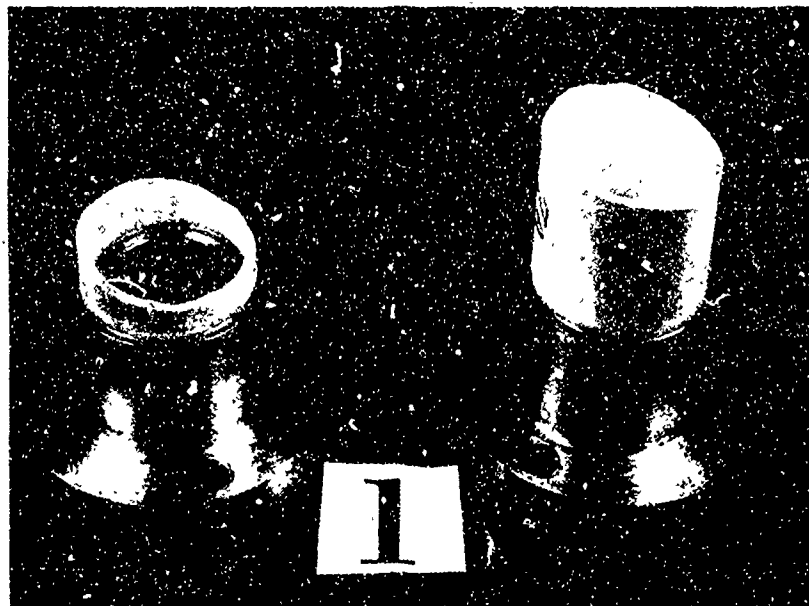


Figure 7. Fractured tube, path 1, Lot 7A, test T1880.

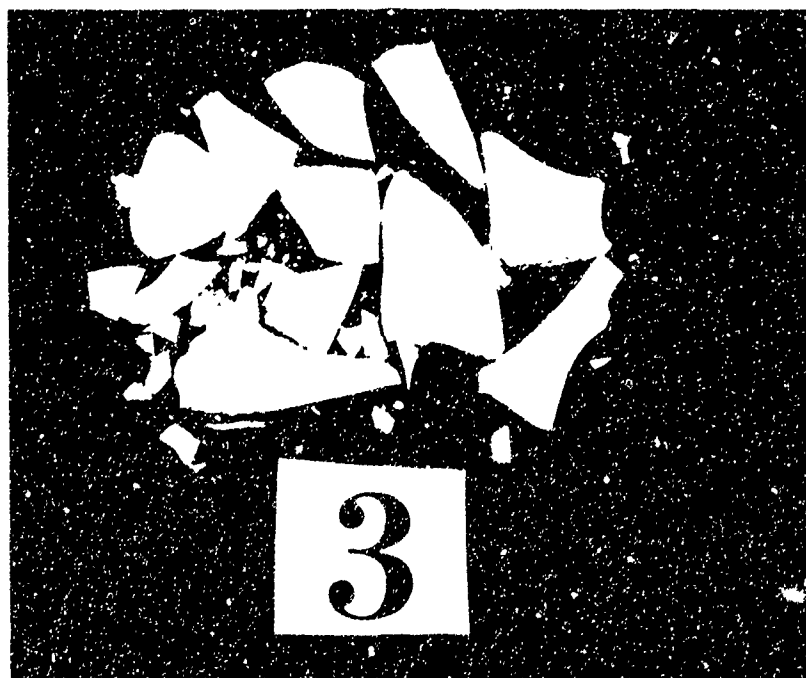


Figure 8a. Fractured tube, path 3, Lot 6A, test T1857.

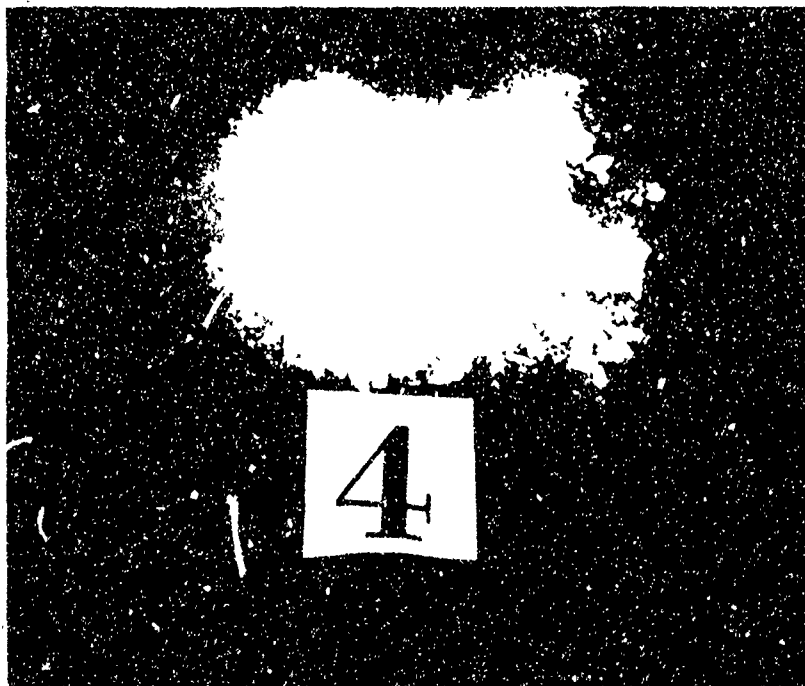


Figure 8b. Fractured tube, path 4, Lot 4A, test T1854.



Figure 8c. Fractured tube, path 5, Lot 5A, test T1846.

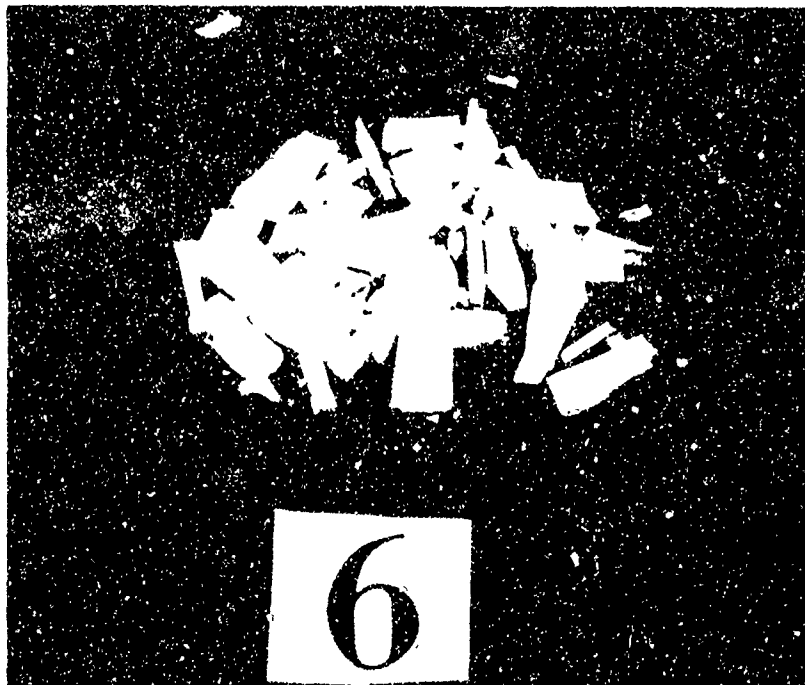


Figure 8d. Fractured tube, path 6, Lot 5A, test T1839.



Figure 9a. Fractured tube, path 7, Lot 6A, test T1871.



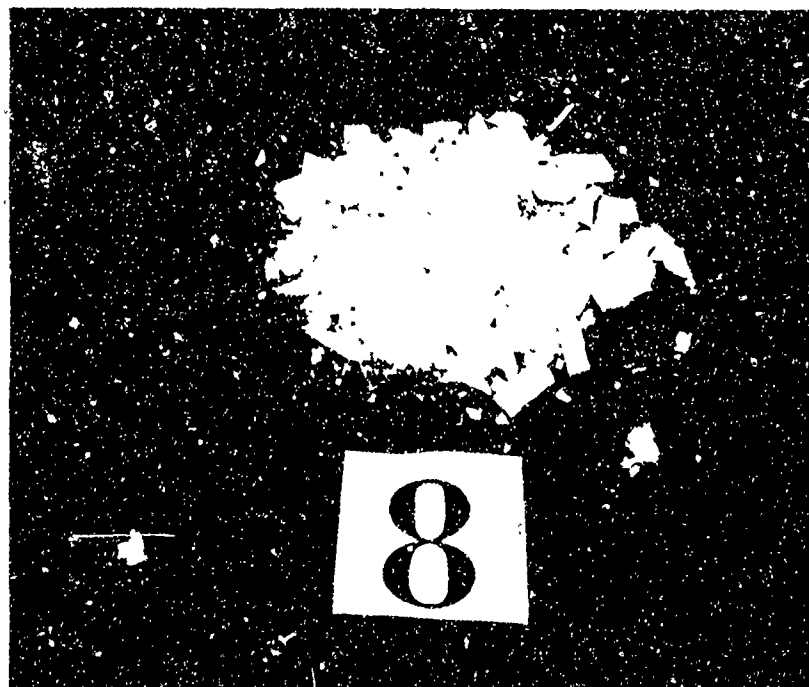


Figure 9b. Fractured tube, path 8, Lot 6A, test T1866.



Figure 9c. Fractured tube, path 9, Lot 6A, test T1849.



Figure 9d. Fractured tube, path 10, Lot 5A, Test T1882.

## REFERENCES

1. Harris, J. N., Welsh, E. A., and Murphy, J. H., Fused Silica Design Manual, Georgia Institute of Technology. Engineering Experiment Station, Naval Ordnance Systems Command, Technical Report No. 4, Contract N00017-70-C-4438, June 1972.
2. Burleson, W. G. and Letson, K. N., Preliminary Thermal Analysis and Design Considerations for the Trace Radome, US Army Missile Command, Redstone Arsenal, Alabama, February 1972, Report No. RL-TM-72-1 (Unclassified).
3. Ely, R. E., "Strength Results for Two Brittle Materials Under Biaxial Stresses," US Army Missile Command, Redstone Arsenal, Alabama, September 1972, Report No. RR-TR-72-11 (Unclassified).
4. Weng, T., "Biaxial Fracture Strength and Mechanical Properties of Graphite-Base Refractory Composites," AIAA Journal, 7, No. 5, May 1969, pp. 851-858.
5. Broutman, L. J., Krishnakumar, S. M., and Mallick, P. K., "Effects of Combined Stresses on Fracture of Alumina and Graphite," J. Amer. Ceramic Soc., 53, No. 12, December 1970, pp. 649-654.
6. Romano, M., "On Leon's Criterion," Meccanica (AIMETA), 4, No. 1, March 1969, pp. 48-66.
7. Cornet, I., and Grassi, R. C., "A Study of Theories of Fracture Under Combined Stresses," J. of Basic Engineering, 83, March 1961, pp. 33-44.
8. Ely, R. E., "Strength of Titania and Aluminum Silicate Under Combined Stresses," J. American Ceramic Society, 55, No. 7, July 1972, pp. 347-350.